GeoHazards

MDPI

Article

Spatial Variations of Physical Characteristics of Soil and Their Role in Creating a Model of a Geogenic Radon Hazard Index (GRHI) in the Kuznetsk Coal Basin

Timofey Leshukov [1,*], Konstantin Legoshchin [1], Maria Savkina [1], Elizaveta Baranova [2], Kirill Avdeev [2] and Aleksey Larionov [2]

[1] Department of Geology and Geography, Institute of Biology, Ecology and Natural Resources, Kemerovo State University, 6 Krasnaya Street, 650000 Kemerovo, Russia; geology@kemsu.ru (K.L.); polina_you_frend@mail.ru (M.S.)
[2] Department of Genetics and Fundamental Medicine, Institute of Biology, Ecology and Natural Resources, Kemerovo State University, 6 Krasnaya Street, 650000 Kemerovo, Russia; laveivana@mail.ru (E.B.); avdeev.burzum@yandex.ru (K.A.); larionov@kemsu.ru (A.L.)
* Correspondence: tvleshukov@kemsu.ru

Abstract: Geographic patterns determine geogenic radon factors that, changing over the territory, form spatial structures of different scales associated with regional and local variations. The study of these structures is important for assessing the possibility of using limited data to predict geogenic radon potential. Our research focuses on the study of the physical properties of soils (moisture, soil density, porosity and void ratio) in the Kuznetsk coal basin. Their variations are studied using statistical methods, a variogram cloud and spatial autocorrelation of data. Soil moisture and porosity have the greatest variability in space and with depth. We conclude that the assessment of geogenic radon predictors requires consideration of the variation coefficient and autocorrelation indices at different scales. Based on the variability of humidity and the fairly homogeneous nature of the studied soils (loams), to assess the radon hazard, it is necessary to study the influence of climatic conditions, since the permeability of the environment for radon will be determined by soil moisture. With the predominance of substantially clayey soils, it is necessary to study the content of ^{226}Ra in the upper horizons, since it is assumed that radon is predominantly diffusely transferred, in which its role is dominant.

Keywords: physical properties of soil; soil moisture; soil density; soil porosity; porosity coefficient; Kuznetsk coal basin; spatial variation; GRHI

Citation: Leshukov, T.; Legoshchin, K.; Savkina, M.; Baranova, E.; Avdeev, K.; Larionov, A. Spatial Variations of Physical Characteristics of Soil and Their Role in Creating a Model of a Geogenic Radon Hazard Index (GRHI) in the Kuznetsk Coal Basin. *GeoHazards* **2024**, *5*, 1294–1307. https://doi.org/10.3390/geohazards5040061

Received: 28 October 2024
Revised: 20 November 2024
Accepted: 2 December 2024
Published: 3 December 2024

1. Introduction

Radon is the second most important factor in the development of human respiratory neoplasms after smoking [1]. Spatial assessment and identification of residential buildings exposed to radon are important for assessing the epidemiological significance of human exposure to radon [2]. Obviously, monitoring in all residential buildings is not possible due to the large number of existing buildings, and only a forecast is available for newly constructed buildings. A solution may be a set of key predictors of radon emission from the geological environment (geogenic radon), while radon influx from other sources can be neglected [3]. Thus, the key factor determining the presence of radon in houses is the geological structure of the territory [4].

Geological predictors of geogenic radon include:

– Concentration of parent elements, including 238U, 235U, 232Th and the precursor 222Rn–226Ra [5]: The main predictor of radon concentration in soils is 226Ra; in rare cases, a significant influence of short-lived decay products of the radioactive series 232Th–220Rn is possible [6,7].

- Physical properties of soils [8,9]: The primary indicators of radon accumulation and migration are soil density, moisture and porosity. They determine the release of radon from soil particles into the cracks and pore spaces of rocks and further migration by diffusion and advection, including emanation onto the daylight surface and into residential buildings. Also very significant is the permeability of rocks for gases, which allows radon to move within the body of the massif or to move to the surface [10–13]. The contribution of permeability depends on the geological situation, since it is important for the possibility of advective transfer of radon, while it is not so important for diffusion.
- The presence of geodynamic zones in the geological environment promotes the active migration of deep gases ("geogases") from horizons deeper than the surface loose sediments to the daylight surface and buildings [14–17].
- Meteorological factors, especially temperature and pressure, usually influence surface radon migration by creating a difference in the temperature and pressure conditions of the rock mass, including between loose rocks, and at the surface layer of the atmosphere [10,18–21]. There is also an increase in radiation exposure at low temperatures due to reduced ventilation of buildings and the "chimney effect".

Not all factors are listed, but it is obvious that the number of predictors of the radon hazard of a territory is large, and it is difficult to measure them all in the process of drawing up a map of the radon hazard in large territories. Therefore, radon concentrations in residential buildings are often predicted using estimates that rely on only a subset of these predictors. For example, the geogenic radon potential (GRP) takes into account the difference in radon concentration at depth and at the surface, as well as the permeability of the geological environment for radon [22–24]. Most often, radon concentration at the surface is not taken into account due to its near-zero value. It is known that these indicators have been studied in a very limited way, even in the areas where radon emanations have been studied. Therefore, the obtained GRP maps have too low a resolution to predict values in residential buildings, and for most areas this is not possible due to a complete lack of data.

Another indicator, the geogenic Rn hazard index (GRHI) [25], can be obtained based on any geogenic indicators available in the region that affect the radon hazard of residential buildings (IRC). Later, a weight of influence was added to each indicator, since in each territory the predictor can have a different effect on the radon hazard. Then, researchers returned to collecting data on local radon predictors and predicting geogenic radon potential based on them. Recently, machine learning (ML) methods have helped in this, which, using large data sets, can provide quite good forecasts of radon hazard, but their accuracy strongly depends on the amount of data, their scale and the variation of the indicator at different spatial levels [26,27].

We can conclude that geogenic radon factors, changing according to geographic patterns, form spatial structures of different scales associated with regional and local variation [28,29]. By studying these structures, at the data collection stage, we can assess the possibilities of using limited data to predict geogenic radon potential. Some indicators may not have large local outliers (called "nuggets" in geostatistics), while other data are very variable, both locally and regionally. Studying these features is important at the regional level, since each region has its own trend of these indicators, to some extent, which depends on its geological history. And this is an important step in making forecasts for large areas. A detailed observation network is required for a thorough study and prediction of GRP and GRHI, but it is not possible due to large financial, labor and time costs. Most often, the data do not have high resolution, and the topological maps in this case also have low predictive value at the local level [29,30]. Thus, our study focuses on exploring regional and local-level spatial patterns for predictors of geogenic radon potential. We used limited indicators of physical properties of soils (density, moisture and porosity) for this reason. It can be noted that the availability of theoretical and experimental field observations confirms the relationship of the parameters we used with respect to radon

and its migration. Another reason is that the parameters we used (density, humidity, porosity and porosity coefficient) are standard for engineering and geological surveys conducted in the Kuznetsk coal basin and Russia according to uniform protocols, which allows us to compare and use these data to assess the physical properties of the soil and their connection with radon. Therefore, these indicators can provide important information at the preliminary stage of radon hazard assessment. On the Russian radon hazard map, the territory of the Altai–Sayan folded region, within which the Kuznetsk coal basin is located, is classified as a dangerous radon zone [31]. According to annual state monitoring data, radon makes the largest contribution to the irradiation of the population of the study area—2.09–3.33 mSv/year (2020–2022)—and the share of residential buildings with excess radon is about 4–5% [32]. These data were obtained by studying 1708 buildings, which very limitedly characterize the impact of radon compared to the total infrastructure stock. A number of studies of this territory obtained very significant concentrations of soil radon, radon flux density and radon concentrations in residential buildings [33–35]. Thus, the geological environment is capable of significantly increasing the radon flux into residential buildings and irradiating the population of the Kuznetsk coal basin.

In this paper, some important characteristics of the Kuznetsk coal basin soils, and their local and regional variations, are demonstrated, since it seems possible to use these data to predict geogenic radon. For the Kuznetsk basin, a step-by-step process of GRP assessment is also important due to its cold climate with a long winter.

2. Materials and Methods

2.1. Characteristics of Cover Deposits of the Kuznetsk Coal Basin

The cover deposits of the Kuznetsk coal basin lie subhorizontally and are represented by loose conglomerate–sand–clay deposits with a thickness of 10–20 to 80–100 m. The age of the deposits is from the Cretaceous to the Quaternary period. The deposits of the Cretaceous and Paleogene periods are very spatially limited and are found only in the north-eastern and south-western parts of Kuzbass. Neogene deposits are more common and are usually represented by lenses and lens-shaped bodies, composed mainly of dense brown and variegated clays with interlayers of sand and pebbles. Quaternary deposits are distributed almost everywhere in the Kuznetsk coal basin with a total thickness of 1 to 80 m. They are represented by deposits of different genetic types (alluvial, diluvial, proluvial, etc.). According to the fractional composition, there are sandy-clayey and gravel–pebble deposits of river valleys [36].

2.2. Characteristics of Local Variation in the Study Area

VAR depth variation was assessed in the central part of the Kuznetsk basin at several points (A and B). The depth of the Paleozoic rocks here is from 10 to 60 m. The composition of loose cover deposits is dominated by clay granulometric size particles, while the uppermost part is represented by loess-like loams corresponding in age to the Upper Pleistocene. For territory A, the distances between the physical properties of soils assessment points varied from 92 to 172 m, with an average distance of 129 m. There were 46 study points in total. In area B, 20 points were studied, which were located from 97 to 150 m apart, with an average distance of 121 m. Also, for both areas, an assessment of the physical properties was made for three boreholes (0.6, 1.0 and 1.5 m), located 5 m apart at each observation point. Thus, we obtained 138 boreholes for area A and 60 boreholes for area B. Clarification of local variation was made for the same depths.

2.3. Regional Variation

For a preliminary assessment of regional variation, 43 sites were studied, in each of which from 3 to 46 boreholes were drilled, located at a distance from each other. Figure 1 shows the locations of these sites within the Kuznetsk coal basin. The physical properties of the soils were averaged in each site and then used to assess regional variation. The figure

shows the locations of the boreholes in the Kuznetsk coal basin. The distance between the territories ranged from 0.2 to 30 km, with an average distance of 6.3 km.

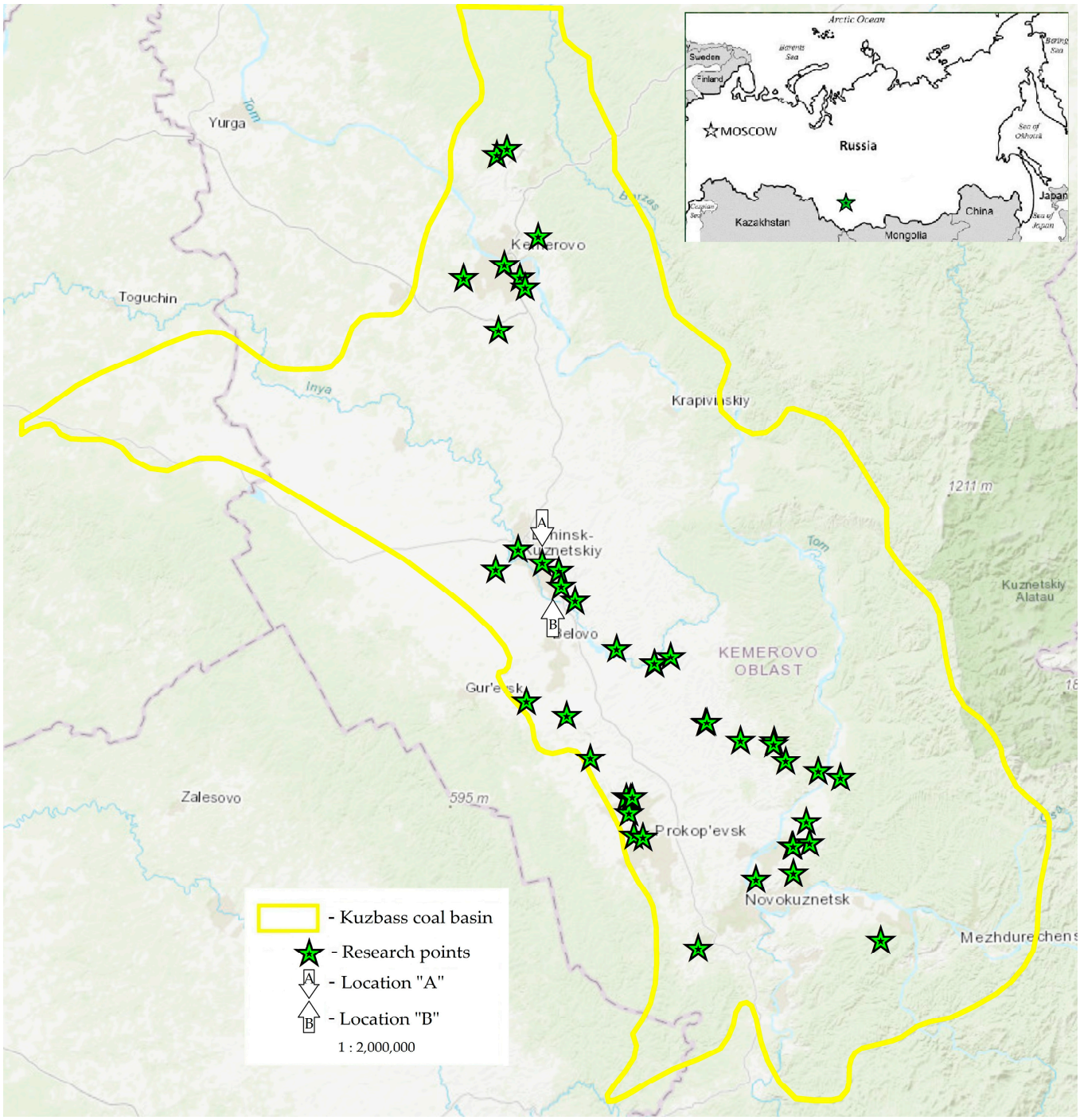

Figure 1. Map of the locations of sites for studying the physical properties of soils in the Kuzbass coal basin.

2.4. Soil Sampling and Physical Soil Assessment

Sampling was into sterile plastic containers with tightly closing lids. For areas A and B, sampling was carried out from depths of 0.6, 1.0 and 1.5 m.

All studies in this section were in accordance with the GOST 5180–2005 standards [37]. The physical soil assessment included moisture (W), soil density (P), dry soil density, soil particle density, porosity (n) and the void ratio/porosity coefficient (e).

Natural moisture was measured by long-term drying of the sample in a drying cabinet at a constant temperature (105 ± 2 °C) with periodic measurement of its mass. Drying was carried out until an insignificant difference in the mass of the soil with the weighing bottle (no more than 0.02 g) was obtained between subsequent mass measurements. Further assessment was carried out using Formula (1) [37]:

$$W = 100 \times \frac{m_1 - m_0}{m_0 - m}, \quad (1)$$

where W is the soil moisture content, %;

m_1 is the mass of wet soil with a weighing bottle, g;

m_0 is the mass of dried soil with a weighing bottle, g;

m is the mass of an empty weighing bottle, g.

The natural density of the soil was measured by weighing a paraffin-coated sample in water. The round sample was weighed on a scale and then covered with heated paraffin. Air bubbles were removed with a heated needle. The paraffin-coated sample was then weighed, and then it was weighed inside a vessel with water, with complete immersion. The density of the sample was then calculated using Formula (2) [37]:

$$P = \frac{m \times p_p \times p_w}{p_p \times (m_1 - m_2) - p_w \times (m_1 - m)}, \quad (2)$$

where m is the mass of the soil sample before paraffin-coating, g;

m_1 is the mass of the paraffin-coated sample, g;

m_2 is the result of weighing the sample in water—the difference between the mass of the paraffin-coated sample and the water displaced by it, g;

p_p is the density of the paraffin, taken to be 0.900 g/cm^3;

p_w is the density of water at the test temperature, g/cm^3.

The density of the skeleton (dry) soil was calculated using data on the natural density and moisture of the sample according to Formula (3) [37]:

$$P_d = \frac{P}{1 + 0.01 \times W}, \quad (3)$$

where P_d is the density of dry soil;

P is the density of the native soil, g/cm^3;

W is the moisture of the soil, %.

The density of the soil particles was estimated using the pycnometric method. The pycnometer, filled one-third with distilled water, was weighed, after which a dried soil sample was added, and it was weighed again. Then, the pycnometer was boiled in a sand bath for 1 h to remove air particles, while adding new amounts of water to the graduation mark. Then, the contents of the pycnometer were poured out, it was rinsed, and distilled water was poured into it and it was kept in a bath with water at the same temperature.

Then the calculations were made using Formula (4) [37]:

$$P_s = \frac{P_w \times m_0}{m_o + m_2 - m_1}, \quad (4)$$

where m_0 is the mass of the dry soil sample, g;

m_1 is the mass of the pycnometer with water and soil after boiling at the test temperature, g;

m_2 is the mass of the pycnometer with water at the same temperature, g;

P_w is the density of water at the same temperature, g/cm^3.

The porosity of the soil was measured considering the density of the soil particles and skeleton (dry) soil using Formula (5) [38]:

$$n = \frac{P_s - P_d}{P_s} \times 100, \quad (5)$$

where P_s is the density of soil particles, g/cm^3;

P_d is the density of dry soil, g/cm^3.

The porosity coefficient describes similar physical properties of the soil, but demonstrates the ratio of the pore volume to the solid phase of the soil. This indicator can be estimated using the following formula.

The porosity coefficient was calculated (6) [38]:

$$e = \frac{P_s - P_d}{P_d} \times 100, \quad (6)$$

where P_s is the density of soil particles, g/cm^3;

P_d is the density of dry soil, g/cm^3.

2.5. Statistical Data Processing

For all data, descriptive statistics were used (mean, standard error, median, minimum, maximum, coefficient of variation, quartile (25% and 75%) and standard deviation) using the statistics program.

Comparison of samples by the physical properties of soils at different depths was performed using the Kruskal–Wallis (K–W) test with the statistical significance level $p < 0.05$, since the data did not correspond to the normal distribution. Spatial patterns were assessed with the spatial autocorrelation data tool "Semivariogram/Covariance Cloud". The basic fundamental assumption of this tool is the law of data stationarity, based on which points located at the same distance and direction from each other should have similar squares of the difference between the values. If the autocorrelation is expressed only in distance, this case refers to isotropy; if in some direction the data are autocorrelated at other distances, then to anisotropy. The data were also tested for the presence of data autocorrelation using the global one-dimensional Moran's index, which evaluates the relationships between indicators at different points in space. The selected methods are standardized for assessing the presence of outliers in the data (presence of "nuggets") and identifying autocorrelation in the data. The presence of "nuggets" suggests the presence of local structures in the data that should be studied at a different, more detailed scale. It was also assumed that the presence of autocorrelation demonstrates the importance of space as a predictor of soil properties. Data can be clustered, when the data can be divided into clusters with different values, or dispersed, when data with high and low values are adjacent. In the case of dispersed data, there are also most likely either random outliers or the presence of smaller structures that should be studied at a larger scale.

3. Results

3.1. Differences in Physical Properties of Soils by Depth at the Local Level

Table 1 presents the results of the study of physical properties of soils at different depths.

The largest coefficient of variation between observation points within both areas is found for soil moisture, followed by the porosity coefficient. The K–W test shows no differences between the three depth groups for the porosity coefficient and soil porosity, but significant differences are found for soil density and moisture. Similar data patterns are characteristic for the compared groups of 1.0 and 1.5 m, as well as for 0.6 and 1.5 m. At the same time, for 0.6 and 1.0 m, there is no difference in soil moisture. A tendency for soil density and moisture to increase with depth is noted for both locations.

Table 1. Physical properties of soils at locations A and B.

		Depth, m	Mean + St. Er.	Median	Min	Max	Coeff. Variation	25% Q	75% Q	St. Deviation
A	P, g/cm^3	0.6	1.77 ± 0.01	1.78	1.40	1.97	5.52	1.74	1.81	0.10
		1	1.81 ± 0.01	1.80	1.70	2.18	4.66	1.76	1.85	0.09
		1.5	1.83 ± 0.01	1.83	1.73	1.93	2.43	1.81	1.87	0.04
	W, %	0.6	6.3 ± 0.6	5.1	1.6	16.8	58.6	3.5	8.9	3.7
		1	5.4 ± 0.5	4.4	1.7	13.9	58.5	2.8	7.5	3.2
		1.5	7.4 ± 0.5	7.3	2.1	19.7	48.4	4.6	9.6	3.6
	e	0.6	60.6 ± 1.7	58.1	39.9	105.8	19.3	53.8	66.8	11.7
		1	56.5 ± 1.3	55.7	26.8	74.0	15.1	52.9	61.5	8.5
		1.5	58.9 ± 1.0	58.3	44.9	77.0	11.1	54.3	62.9	6.5
	n	0.6	37.4 ± 0.6	36.7	28.5	51.4	11.3	35.0	40.1	4.2
		1	35.9 ± 0.5	35.8	21.1	42.5	10.3	34.6	38.1	3.7
		1.5	36.9 ± 0.4	36.8	31.0	43.5	6.9	35.2	38.6	2.5
B	P, g/cm^3	0.6	1.78 ± 0.01	1.77	1.66	1.93	3.44	1.74	1.82	0.06
		1	1.81 ± 0.01	1.81	1.71	1.96	3.37	1.78	1.85	0.06
		1.5	1.84 ± 0.02	1.83	1.73	2.08	4.48	1.81	1.88	0.08
	W, %	0.6	6.2 ± 0.6	6.1	1.6	10.1	42.7	3.8	8.4	2.6
		1	6.7 ± 0.5	6.7	3.1	11.1	33.3	5.1	8.3	2.2
		1.5	8.3 ± 0.8	7.7	2.9	18.0	41.4	6.2	10.2	3.4
	e	0.6	59.8 ± 1.4	58.5	50.3	73.1	10.6	55.5	64.7	6.3
		1	58.4 ± 1.5	56.5	46.0	72.4	11.6	54.8	62.9	6.8
		1.5	59.4 ± 2.0	58.4	43.2	84.7	15.3	54.3	63.3	9.1
	n	0.6	37.3 ± 0.5	36.9	33.5	42.2	6.5	35.7	39.3	2.4
		1	36.8 ± 0.6	36.1	31.5	42.0	7.2	35.4	38.6	2.7
		1.5	37.1 ± 0.8	36.9	30.2	45.9	9.4	35.2	38.8	3.5

3.2. Spatial Variations of Data at the Local Level

The spatial structural features of the data were studied using spatial autocorrelation, and the results are presented in Table 2.

Table 2. Spatial autocorrelation of physical properties of soils at different depths in areas A and B.

		Depth, m	Observed	Expected	St. Deviation	z-Score	*p*-Value
A	P	0.6	−0.047	−0.022	0.017	−0.187	0.85
		1	0.060		0.016	0.656	0.51
		1.5	0.223		0.019	1.787	0.07 *
	W	0.6	0.312		0.019	2.451	0.01 *
		1	0.382		0.018	2.979	<0.01 *
		1.5	0.222		0.018	1.826	0.07 *
	e	0.6	−0.005		0.017	0.129	0.90
		1	0.016		0.018	0.284	0.78
		1.5	0.296		0.018	2.350	0.02 *
	n	0.6	0.004		0.018	0.198	0.84
		1	0.038		0.017	0.468	0.64
		1.5	0.309		0.018	2.436	0.02 *
B	P	0.6	−0.572	−0.053	0.036	−2.741	0.01 **
		1	−0.094		0.037	−0.213	0.83
		1.5	0.135		0.032	1.046	0.30
	W	0.6	−0.021		0.039	0.161	0.87
		1	−0.224		0.038	−0.878	0.38
		1.5	−0.203		0.034	−0.824	0.41
	e	0.6	−0.530		0.038	−2.456	0.01 **
		1	−0.083		0.037	−0.157	0.88
		1.5	0.168		0.033	1.213	0.23
	n	0.6	−0.536		0.038	−2.475	0.01 **
		1	−0.081		0.037	−0.146	0.88
		1.5	0.183		0.034	1.270	0.20

*—clustered, **—dispersed.

Some spatial ordering is revealed by the formation of cluster structures and the disruption of clustering in the form of dispersion structures. Most of the results are characterized by indices indistinguishable from a random distribution of data.

3.3. Spatial Features of the Physical Properties of Soils at the Regional Level

Based on the smallest variation coefficient for 1.5–2 m depth, we compared territories significantly distant from each other; these data are presented in Table 3.

Table 3. Physical properties of soils for the entire region of the Kuznetsk coal basin.

		Mean + St. Er.	Median	Min	Max	Coeff. Variation	25% Q	75% Q	St. Deviation
All territory	P, g/cm^3	1.94 ± 0.01	1.94	1.77	2.13	3.65	1.89	1.99	0.07
	W, %	20.3 ± 0.9	21.3	7.4	32.0	29.1	16.0	25.3	5.9
	e	67.0 ± 1.7	66.7	36.9	97.6	21.9	57.5	77.7	14.7
	n	38.3 ± 2.2	37.2	21.7	74.4	30.0	30.5	42.9	11.5

Lower soil moisture variation coefficients are noted, while the porosity coefficient and soil porosity increase at the regional scale of the study.

In general, for the studied data, within each studied territory there are also local variations in the physical properties of soils. The coefficient of variation for moisture content ranged from 3% to 59%, for soil density from approximately 0.7% to 17.5%, for porosity from approximately 0.8% to 110%, and for the porosity coefficient from 1.6% to 65.6%. The variogram cloud for the data is shown in Figure 2.

The variograms can show local outliers (nuggets), which can be errors or important artifacts of local data variation.

The spatial autocorrelation assessment is presented in Table 4.

Table 4. Spatial autocorrelation of data at the regional level.

		Observed	Expected	St. Deviation	z-Score	*p*-Value
All territory	P	0.311	−0.024	0.061	1.359	0.17
	W	0.160		0.062	0.740	0.46
	e	0.224		0.062	0.999	0.32
	n	0.218		0.058	1.006	0.31

At the regional level, regular spatial structures of data were not obtained; the distribution of values is chaotic.

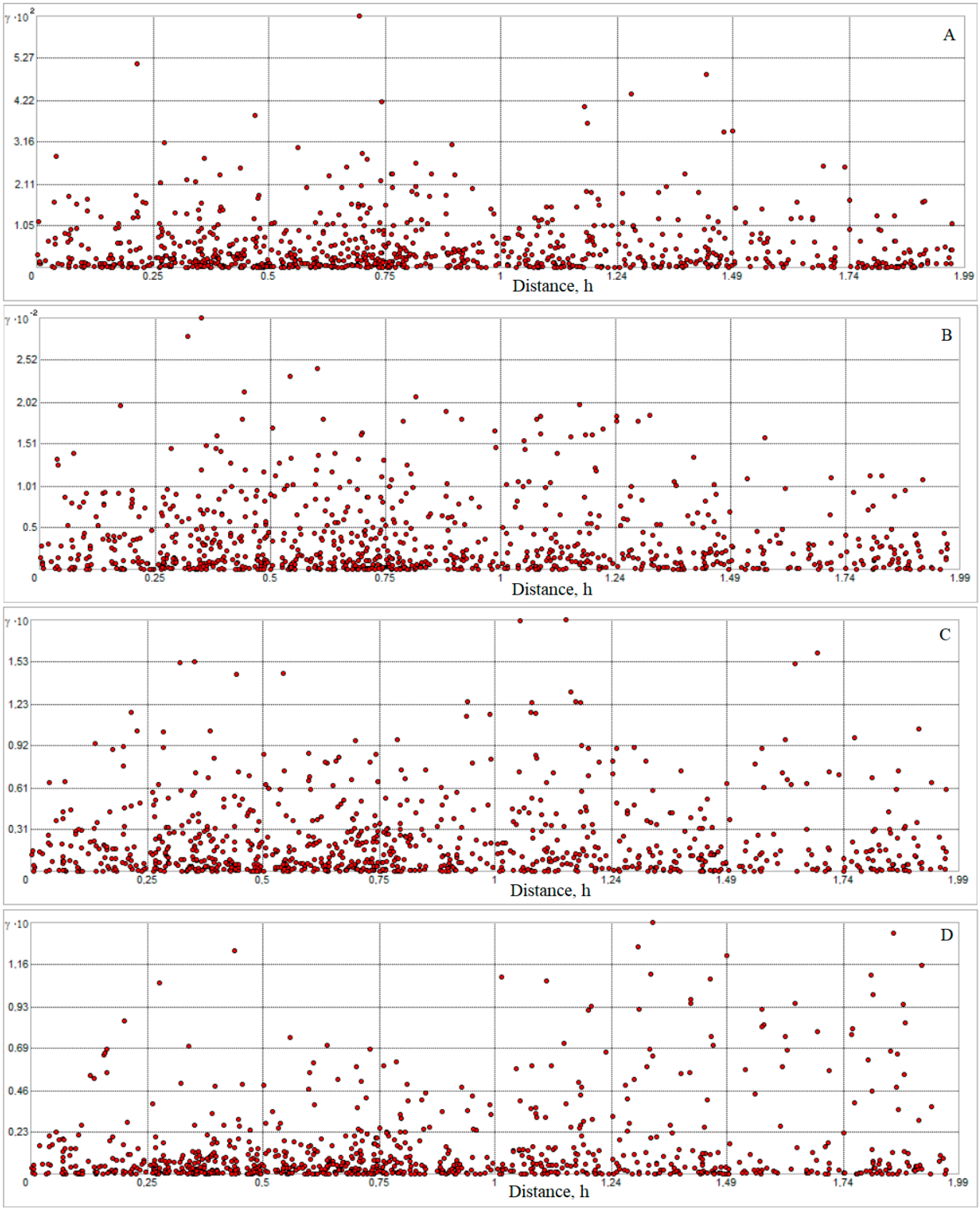

Figure 2. Variograms of physical properties of soils at the regional level. (**A**) density, (**B**) moisture, (**C**) porosity coefficient and (**D**) soil porosity.

4. Discussion

According to our data, the physical properties of soils have some variability in relation to depth. For both areas (A and B), the humidity and density of the soil increased with depth, but the porosity remained almost unchanged. Usually, soils are characterized by an increase in the humidity and density of the soil, as well as a decrease in porosity and the porosity coefficient with depth.

The absence of statistically significant differences in soil moisture at depths of 0.6 and 1 m, with overall low moisture, is most likely due to the small amount of precipitation during the study period, which were the conditions during our experiment. The waters in this zone are mainly represented by hygroscopic and surface film water, but, deeper, the role of free water (capillary and gravitational) increases. Low density indicators in some samples are a consequence of the uneven depth of the base of the decompressed upper-layer soil; in this case, soil particles got into the sample, which significantly reduced the density of the sample. The moisture content of soils usually reduces the possibility of radon diffusion. An increase in porosity, simultaneously with an unchanged humidity index, leads to a decrease in the proportion of pores occupied by water. Under these conditions, radon can migrate quite freely.

In agreement with the results of previous works, the properties of the soil affect the processes of accumulation and migration of radon in it [39–41]. The upper soil layer (up to 1 m, depending on the type of soil) is characterized by a better ability to release radon to the daylight surface due to its higher porosity and its dependence on the gradient of thermobaric conditions between the ground layer and the soil air [42,43]. Soil moisture also can affect the decrease or increase of radon exhalation from the soil [44,45]. Increased migration occurs due to the decrease of radon sorption on the surface of wet soil particles. When the volume of moisture increases even more and it closes the crack/pore space for radon migration, its emission decreases. In this paper, we conclude that low soil moisture, high porosity and a high porosity coefficient contribute to the removal of radon from the soil from depths of up to 1 m and, according to this, the concentration of radon will probably increase deeper. In general, loosening and decreasing the moisture content of soils closer to the surface leads to a better connection between the thermobaric conditions of the soil air and the surface atmosphere; this leads to better migration activity of radon. This is indirectly confirmed by a large number of studies in which the concentration of radon increases with depth and its daily and seasonal cycles are clearly expressed, correlating with meteorological conditions [18,20].

Soil moisture at all depths has a very high variability across different study locations. This indicator will be important for mapping radon potential at the local level and extrapolating to regional radon hazard forecasting. Such spatial variability at the local level can significantly and randomly affect the final result at all scales [26].

Climate conditions significantly affect the average annual radon emission to the surface [46]. Within the Kuzbass, precipitation varies from less than 400 mm to approximately 700 mm per year with a maximum in summer. Humidity has a significant impact on radon migration in soils, which leads to a significant decrease in the quality of radon hazard prediction based on permeability [11].

The study area is characterized by predominantly loamy soils, in which radon diffusion dominates, and convection as a migration method is hampered by low permeability [47,48]. In this case, permeability will increase with the activation of tectonic processes, which will lead to the formation of fault structures. Fault zones obviously affect such processes [49–51]. Otherwise, the radon flux to the surface will depend on the concentration of ^{226}Ra in the upper soil layer; as is known, diffusion is very limited by distance. It is also known that the emanation coefficient of rocks is partially inversely dependent on grain size [11], which is to be expected in our case, since the size of soil particles is quite small.

Extremely low variability of soil density in natural soil composition at the local level is noted for both territories. For territory A, the variation coefficient decreases with depth, while for territory B, on the contrary, it increases. Thus, different local geological conditions

can lead to differences in soil density in different horizons. Clustering of data for territory A by soil moisture at all depths and clustering of data by density, porosity and porosity coefficient for depths of 1.5 m suggest the presence of a cluster of soils with similar moisture content and other properties that are distinguishable from the rest of the territory. The presence of such spatially clustered data for a small study area suggests that local conditions must be taken into account in the spatial analysis of the physical properties of soils.

Spatial dispersion patterns of the data for area B for soil density, porosity and void ratio at depths of 0.6 m indicate the presence of strong lateral differences/gradients of these parameters, which are common in this location, compared to random occurrence. If we note the small distance between observation points, most likely, there is spatial variation of these properties on a smaller scale. There is an increase in the coefficient of variation of average porosity values and the porosity coefficient at the regional level, while these data do not form any spatial structures (cluster or dispersion). Lower variability of the soil moisture indicator is also noted.

Our research is limited by the amount of data used in the regional assessment, as follows from Figure 1, which indicates the unevenness of the data in space. In this regard, it is necessary to increase the amount of data, striving for a more uniform distribution in space. However, the existing data are concentrated in the main locations of residence of the population in the coal basin and can be used to assess geogenic radon without losing the accuracy of the model for these areas. Studying the physical properties of soils for Quaternary deposits, which almost completely cover more ancient rocks and dominate the geological environment of the Kuzbass cover deposits, will allow us to approach the construction of a relevant map of the radon hazard of the territory. It is considered that it is the upper horizons of the lithosphere, their physical and radiogenic properties, that determine the radon hazard of the territory, especially for geodynamically quiet territories [52]. The presented data allow us to formulate the directions of further research. Based on the dominant composition of soils (mainly loams), we understand that the main force of radon movement will be diffusion, and the radon level in this case mainly depends on the content of ^{226}Ra in the soils.

5. Conclusions

In this paper, we studied the features of vertical variation of physical properties of soil, which differed in density and moisture, but not in porosity and the porosity coefficient. Spatially, local clusters were found, and the data showed autocorrelation. This study demonstrates that when assessing the spatial homogeneity of data and their quality, it is necessary to consider the coefficients of variation and autocorrelation indices at different scales, which are affected by local effects. In this case, when assessing the significance of predictors of radon concentration in soils and its migration (physical properties of the soil in our case), it is necessary to take into account the presence of geographic local structures, which implies the use of geographically weighted regression (GWR). The use of this method is beyond the scope of our study, but in the future it will help us to demonstrate spatial associations between physical properties of soils, alongside other predictors, and the radon hazard of the territory. Based on the variability of humidity and the fairly homogeneous nature of the studied soils (loams), to assess the radon hazard, it is necessary to study the influence of climatic conditions (precipitation volume) of the Kuznetsk coal basin, since the permeability of the environment for radon will be determined by soil moisture. With the predominance of substantially clayey soils, it is necessary to study the content of ^{226}Ra in the upper horizons, since it is assumed that radon is predominantly diffusely transferred, in which its role is dominant.

Author Contributions: Conceptualization, T.L. and A.L.; methodology, T.L.; software, T.L.; validation, K.L., T.L., K.A., E.B., M.S. and A.L.; formal analysis, T.L. and A.L.; investigation, K.L., T.L., K.A., E.B., M.S. and A.L.; resources, T.L. and A.L.; data curation, T.L.; writing—original draft preparation, T.L. and A.L.; writing—review and editing, K.L., T.L. and A.L.; visualization, T.L.; supervision,

T.L.; project administration, A.L.; funding acquisition, A.L. All authors have read and agreed to the published version of the manuscript.

Funding: This research was funded by the Russian Science Foundation (RSF), under research project No. 23-27-00320, https://rscf.ru/en/project/23-27-00320/ (accessed on 30 September 2024).

Data Availability Statement: The original contributions presented in the study are included in the article, further inquiries can be directed to the corresponding author.

Conflicts of Interest: The authors declare no conflicts of interest.

References

1. Riudavets, M.; Garcia de Herreros, M.; Besse, B.; Mezquita, L. Radon and Lung Cancer: Current Trends and Future Perspectives. *Cancers* **2022**, *14*, 3142. [CrossRef] [PubMed]
2. Pasculli, A.; Palermi, S.; Sarra, A.; Piacentini, T.; Miccadei, E. A Modelling Methodology for the Analysis of Radon Potential Based on Environmental Geology and Geographically Weighted Regression. *Environ. Model. Softw.* **2014**, *54*, 165–181. [CrossRef]
3. Appleton, J.D.; Miles, J.C.H. A Statistical Evaluation of the Geogenic Controls on Indoor Radon Concentrations and Radon Risk. *J. Environ. Radioact.* **2010**, *101*, 799–803. [CrossRef] [PubMed]
4. Chen, J.; Ford, K.L. A Study on the Correlation between Soil Radon Potential and Average Indoor Radon Potential in Canadian Cities. *J. Environ. Radioact.* **2017**, *166*, 152–156. [CrossRef]
5. Demoury, C.; Ielsch, G.; Hemon, D.; Laurent, O.; Laurier, D.; Clavel, J.; Guillevic, J. A Statistical Evaluation of the Influence of Housing Characteristics and Geogenic Radon Potential on Indoor Radon Concentrations in France. *J. Environ. Radioact.* **2013**, *126*, 216–225. [CrossRef]
6. Voltattorni, N.; Gasparini, A.; Galli, G. The Analysis of 222Rn and 220Rn Natural Radioactivity for Local Hazard Estimation: The Case Study of Cerveteri (Central Italy). *Int. J. Environ. Res. Public Health* **2023**, *20*, 6420. [CrossRef] [PubMed]
7. Hasan, M.M.; Janik, M.; Pervin, S.; Iimoto, T. Preliminary Population Exposure to Indoor Radon and Thoron in Dhaka City, Bangladesh. *Atmosphere* **2023**, *14*, 1067. [CrossRef]
8. Shweikani, R.; Giaddui, T.G.; Durrani, S.A. The Effect of Soil Parameters on the Radon Concentration Values in the Environment. *Radiat. Meas.* **1995**, *25*, 581–584. [CrossRef]
9. Lawrence, C.E.; Akber, R.A.; Bollhöfer, A.; Martin, P. Radon-222 Exhalation from Open Ground on and around a Uranium Mine in the Wet-Dry Tropics. *J. Environ. Radioact.* **2009**, *100*, 1–8. [CrossRef]
10. Miklyaev, P.S.; Petrova, T.B.; Shchitov, D.V.; Sidyakin, P.A.; Murzabekov, M.A.; Tsebro, D.N.; Marennyy, A.M.; Nefedov, N.A.; Gavriliev, S.G. Radon Transport in Permeable Geological Environments. *Sci. Total Environ.* **2022**, *852*, 158382. [CrossRef]
11. Benavente, D.; Valdés-Abellán, J.; Pla, C.; Sanz-Rubio, E. Estimation of Soil Gas Permeability for Assessing Radon Risk Using Rosetta Pedotransfer Function Based on Soil Texture and Water Content. *J. Environ. Radioact.* **2019**, *208–209*, 105992. [CrossRef] [PubMed]
12. Lu, S.-F.; Han, Z.-J.; Xu, L.; Lan, T.-G.; Wei, X.; Zhao, T.-Y. On Measuring Methods and Influencing Factors of Air Permeability of Soils: An Overview and a Preliminary Database. *Geoderma* **2023**, *435*, 116509. [CrossRef]
13. Gil-Oncina, S.; Valdes-Abellan, J.; Pla, C.; Benavente, D. Estimation of the Radon Risk Under Different European Climates and Soil Textures. *Front. Public Health* **2022**, *10*, 794557. [CrossRef]
14. Etiope, G.; Lombardi, S. Laboratory Simulation of Geogas Microbubble Flow. *Geo* **1996**, *27*, 226–232. [CrossRef]
15. Etiope, G.; Martinelli, G. Migration of Carrier and Trace Gases in the Geosphere: An Overview. *Phys. Earth Planet. Inter.* **2002**, *129*, 185–204. [CrossRef]
16. Chen, X.; Liu, Y.; Jiang, Y.; Feng, S. Radon Transport Carried by Geogas: Prediction Model. *Environ. Sci. Pollut. Res.* **2023**, *30*, 86656–86675. [CrossRef]
17. Voltattorni, N.; Sciarra, A.; Quattrocchi, F. The Application of Soil Gas Technique to Geothermal Exploration:Study of "Hidden" Potential Geothermal Systems. In Proceedings of the World Geothermal Congress, Bali, Indonesia, 25–29 April 2010.
18. Benkovitz, A.; Zafrir, H.; Reuveni, Y. A Novel Assessment of the Surface Heat Flux Role in Radon (Rn-222) Gas Flow within Subsurface Geological Porous Media. *Remote Sens.* **2023**, *15*, 4094. [CrossRef]
19. Siino, M.; Scudero, S.; Cannelli, V.; Piersanti, A.; D'Alessandro, A. Multiple Seasonality in Soil Radon Time Series. *Sci. Rep.* **2019**, *9*, 8610. [CrossRef]
20. Haquin, G.; Zafrir, H.; Ilzycer, D.; Weisbrod, N. Effect of Atmospheric Temperature on Underground Radon: A Laboratory Experiment. *J. Environ. Radioact.* **2022**, *253–254*, 106992. [CrossRef]
21. Dueñas, C.; Pérez, M.; Fernández, M.C.; Carretero, J. Radon Concentrations in Surface Air and Vertical Atmospheric Stability of the Lower Atmosphere. *J. Environ. Radioact.* **1996**, *31*, 87–102. [CrossRef]
22. Szabó, K.Z.; Jordan, G.; Horváth, Á.; Szabó, C. Mapping the Geogenic Radon Potential: Methodology and Spatial Analysis for Central Hungary. *J. Environ. Radioact.* **2014**, *129*, 107–120. [CrossRef] [PubMed]
23. Kropat, G.; Bochud, F.; Murith, C.; Palacios (Gruson), M.; Baechler, S. Modeling of Geogenic Radon in Switzerland Based on Ordered Logistic Regression. *J. Environ. Radioact.* **2017**, *166*, 376–381. [CrossRef] [PubMed]

24. Giustini, F.; Ciotoli, G.; Rinaldini, A.; Ruggiero, L.; Voltaggio, M. Mapping the Geogenic Radon Potential and Radon Risk by Using Empirical Bayesian Kriging Regression: A Case Study from a Volcanic Area of Central Italy. *Sci. Total Environ.* **2019**, *661*, 449–464. [CrossRef] [PubMed]
25. Bossew, P.; Cinelli, G.; Ciotoli, G.; Crowley, Q.G.; De Cort, M.; Elío Medina, J.; Gruber, V.; Petermann, E.; Tollefsen, T. Development of a Geogenic Radon Hazard Index—Concept, History, Experiences. *Int. J. Environ. Res. Public Health* **2020**, *17*, 4134. [CrossRef] [PubMed]
26. Gavriliev, S.; Petrova, T.; Miklyaev, P.; Karfidova, E. Predicting Radon Flux Density from Soil Surface Using Machine Learning and GIS Data. *Sci. Total Environ.* **2023**, *903*, 166348. [CrossRef]
27. Petermann, E.; Bossew, P.; Kemski, J.; Gruber, V.; Suhr, N.; Hoffmann, B. Development of a High-Resolution Indoor Radon Map Using a New Machine Learning-Based Probabilistic Model and German Radon Survey Data. *Environ. Health Perspect* **2024**, *132*, 97009. [CrossRef]
28. Coletti, C.; Ciotoli, G.; Benà, E.; Brattich, E.; Cinelli, G.; Galgaro, A.; Massironi, M.; Mazzoli, C.; Mostacci, D.; Morozzi, P.; et al. The Assessment of Local Geological Factors for the Construction of a Geogenic Radon Potential Map Using Regression Kriging. A Case Study from the Euganean Hills Volcanic District (Italy). *Sci. Total Environ.* **2022**, *808*, 152064. [CrossRef]
29. Cinelli, G.; Tollefsen, T.; Bossew, P.; Gruber, V.; Bogucarskis, K.; De Felice, L.; De Cort, M. Digital Version of the European Atlas of Natural Radiation. *J. Environ. Radioact.* **2019**, *196*, 240–252. [CrossRef]
30. Elío, J.; Cinelli, G.; Bossew, P.; Gutiérrez-Villanueva, J.L.; Tollefsen, T.; De Cort, M.; Nogarotto, A.; Braga, R. The First Version of the Pan-European Indoor Radon Map. *Nat. Hazards Earth Syst. Sci.* **2019**, *19*, 2451–2464. [CrossRef]
31. Maksimovskij, V.A.; Reshetov, V.V.; Harlamov, M.G. Radon Hazard Map of Russia 1995. Available online: https://www.researchgate.net/figure/Radon-hazard-map-of-Russia-for-1995-86_fig18_377548215 (accessed on 25 September 2024).
32. *On the State of Sanitary and Epidemiological Well-Being of the Population in the Kemerovo Region—Kuzbass in 2023*; Federal Service for Supervision of Consumer Rights Protection and Human Wellbeing, Office of the Federal Service for Supervision of Consumer Rights Protection and Human Wellbeing in the Kemerovo Region—Kuzbass: Kemerovo, Russia, 2024.
33. Leshukov, T.; Larionov, A.; Legoshchin, K.; Lesin, Y.; Yakovleva, S. The Assessment of Radon Emissions as Results of the Soil Technogenic Disturbance. *Int. J. Environ. Res. Public Health* **2020**, *17*, 9268. [CrossRef]
34. Leshukov, T.; Legoshchin, K.; Larionov, A. Radon Hazard of the Zhurinsky Fault for the Population in the Kuznetsk Coal Basin: Primary Results. *Sustainability* **2023**, *15*, 16774. [CrossRef]
35. Leshukov, T.; Legoshchin, K.; Larionov, A. A Case Study of the Radon Hazard at the Boundary of a Coal Minefield. *Appl. Sci.* **2023**, *13*, 13188. [CrossRef]
36. Cherkas, O. Morphostructural Zoning of the Kuznetsk Depression as a Basis for Creating Applied Maps. Candidate's Thesis, V.S. Sobolev Institute of Geology and Mineralogy of the Siberian Branch of the RAS, Novosibirsk, Russia, 2015.
37. *GOST 5180–2015*; SOILS Laboratory Methods for Determining Physical Characteristics. Interstate Council for Standardization, Metrology and Certification (ISC): Moscow, Russia, 2016.
38. *GOST 25100–2011*; Soils. Classification: Moscow, Russia, 2018.
39. Cecconi, A.; Verginelli, I.; Baciocchi, R. Assessing Light Non-Aqueous Phase Liquids in the Subsurface Using the Soil Gas Rn Deficit Technique: A Literature Overview of Field Studies. *Sustainability* **2024**, *16*, 3317. [CrossRef]
40. Nazaroff, W.W. Radon Transport from Soil to Air. *Rev. Geophys.* **1992**, *30*, 137–160. [CrossRef]
41. Markkanen, M.; Arvela, H. Radon Emanation from Soils. *Radiat. Prot. Dosim.* **1992**, *45*, 269–272. [CrossRef]
42. Benkovitz, A.; Zafrir, H.; Reuveni, Y. The Dynamics of Rn-222 Cyclic Flow within the Shallow Geological Subsurface Media as a Daily Temporal Variated Source for Exhalation into the Air. *Sci. Total Environ.* **2024**, *912*, 169244. [CrossRef]
43. Catalano, R.; Immé, G.; Mangano, G.; Morelli, D.; Aranzulla, M.; Giammanco, S.; Thinova, L. In Situ and Laboratory Measurements for Radon Transport Process Study. *J. Radioanal. Nucl. Chem.* **2015**, *306*, 673–684. [CrossRef]
44. Yang, J.; Busen, H.; Scherb, H.; Hürkamp, K.; Guo, Q.; Tschiersch, J. Modeling of Radon Exhalation from Soil Influenced by Environmental Parameters. *Sci. Total Environ.* **2019**, *656*, 1304–1311. [CrossRef]
45. Benavente, D.; Pla, C. Effect of Pore Structure and Moisture Content on Gas Diffusion and Permeability in Porous Building Stones. *Mater. Struct.* **2018**, *51*, 21. [CrossRef]
46. Galiana-Merino, J.J.; Gil-Oncina, S.; Valdes-Abellan, J.; Soler-Llorens, J.L.; Benavente, D. RadonPotential: An Interactive Web Application for Radon Potential Prediction under Different Climates and Soil Textures. *Earth Sci. Inform.* **2024**, *17*, 2775–2789. [CrossRef]
47. Nunes, L.J.R.; Curado, A.; Lopes, S.I. The Relationship between Radon and Geology: Sources, Transport and Indoor Accumulation. *Appl. Sci.* **2023**, *13*, 7460. [CrossRef]
48. Kashif, M.; Cao, Y.; Yuan, G.; Asif, M.; Javed, K.; Mendez, J.N.; Khan, D.; Miruo, L. Pore Size Distribution, Their Geometry and Connectivity in Deeply Buried Paleogene Es1 Sandstone Reservoir, Nanpu Sag, East China. *Pet. Sci.* **2019**, *16*, 981–1000. [CrossRef]
49. Utkin, V.I.; Yurkov, A.K. Radon as a Tracer of Tectonic Movements. *Russ. Geol. Geophys.* **2010**, *51*, 220–227. [CrossRef]
50. Seminskii, K.; Bobrov, A.A.; Sodnomsambuu, D. Relationship between Radon and the Tectonic Activity of Faults in Central Mongolia. *Dokl. Earth Sci.* **2019**, *487*, 890–893. [CrossRef]

51. Benà, E.; Ciotoli, G.; Ruggiero, L.; Coletti, C.; Bossew, P.; Massironi, M.; Mazzoli, C.; Mair, V.; Morelli, C.; Galgaro, A.; et al. Evaluation of Tectonically Enhanced Radon in Fault Zones by Quantification of the Radon Activity Index. *Sci. Rep.* **2022**, *12*, 21586. [CrossRef]
52. Gavriliev, S.; Petrova, T.; Miklyaev, P. Factors Influencing Radon Transport in the Soils of Moscow. *Environ. Sci. Pollut. Res.* **2022**, *29*, 88606–88617. [CrossRef] [PubMed]